

Vibrating soap films: An analog for quantum chaos on billiards

E. Arcos, G. Báez, P. A. Cuatlayol, M. L. H. Prian, R. A. Méndez-Sánchez,^{a)}
and H. Hernández-Saldaña

Laboratorio de Cuernavaca, Instituto de Física, University of Mexico (UNAM), A. P. 20-364, C. P. 01000,
México, D. F., Mexico and Facultad de Ciencias, UNAM, University of Mexico (UNAM), 04510,
México, D. F., Mexico

(Received 25 June 1996; accepted 10 November 1997)

We present an experimental setup based on the normal modes of vibrating soap films which shows quantum features of integrable and chaotic billiards. In particular, we obtain the so-called *scars*—narrow linear regions with high probability along classical periodic orbits—for the classically chaotic billiards. We show that these scars are also visible at low frequencies. Finally, we suggest some applications of our experimental setup in other related two-dimensional wave phenomena.

© 1998 American Association of Physics Teachers.

I. INTRODUCTION

In recent years, there has been increasing interest in the properties of quantum systems whose classical analogs are chaotic.¹⁻⁴ Part of the work in this new field, called quantum chaos,⁴ refers to essentially two-dimensional cavities or wells of infinite potential called billiards. These billiards can take different forms, such as rectangles, circles, and other more complicated geometries (see Fig. 1). The circle and the rectangle correspond to integrable systems.⁴ Furthermore, we include in Fig. 1 the so-called Bunimovich stadium and the Sinai billiard, which are completely chaotic.⁵ However, in-

termediate situations, i.e., systems with both integrable and chaotic behaviors, are the most common type of dynamical systems.⁶

The quantum analog of a classical billiard is called a quantum billiard and its eigenfunctions are closely related to the classical features of the billiard.⁷ Quantum billiards obey the Helmholtz equation with vanishing amplitude on the border (homogeneous Dirichlet boundary conditions). Such systems can be simulated as a drum or any other membrane vibrating in a frame. The principal purpose of this paper is to show that the quantum behavior of classically chaotic and inte-

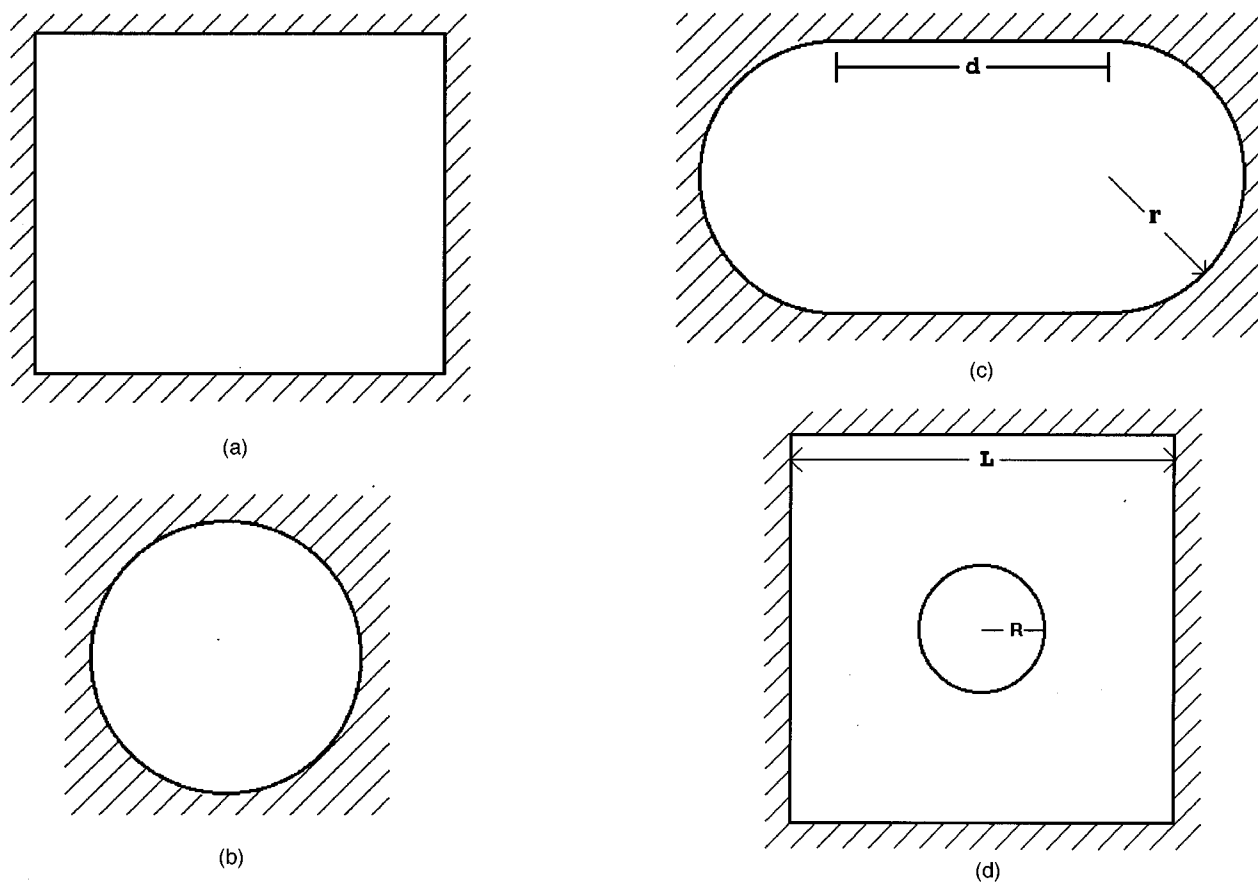


Fig. 1. Integrable billiards: (a) rectangular and (b) circular. Chaotic billiards: (c) the Bunimovich stadium, formed by two semicircles of radius r joined by two segments of length d ; (d) the Sinai billiard, formed by a square with a circle of radius R inside.

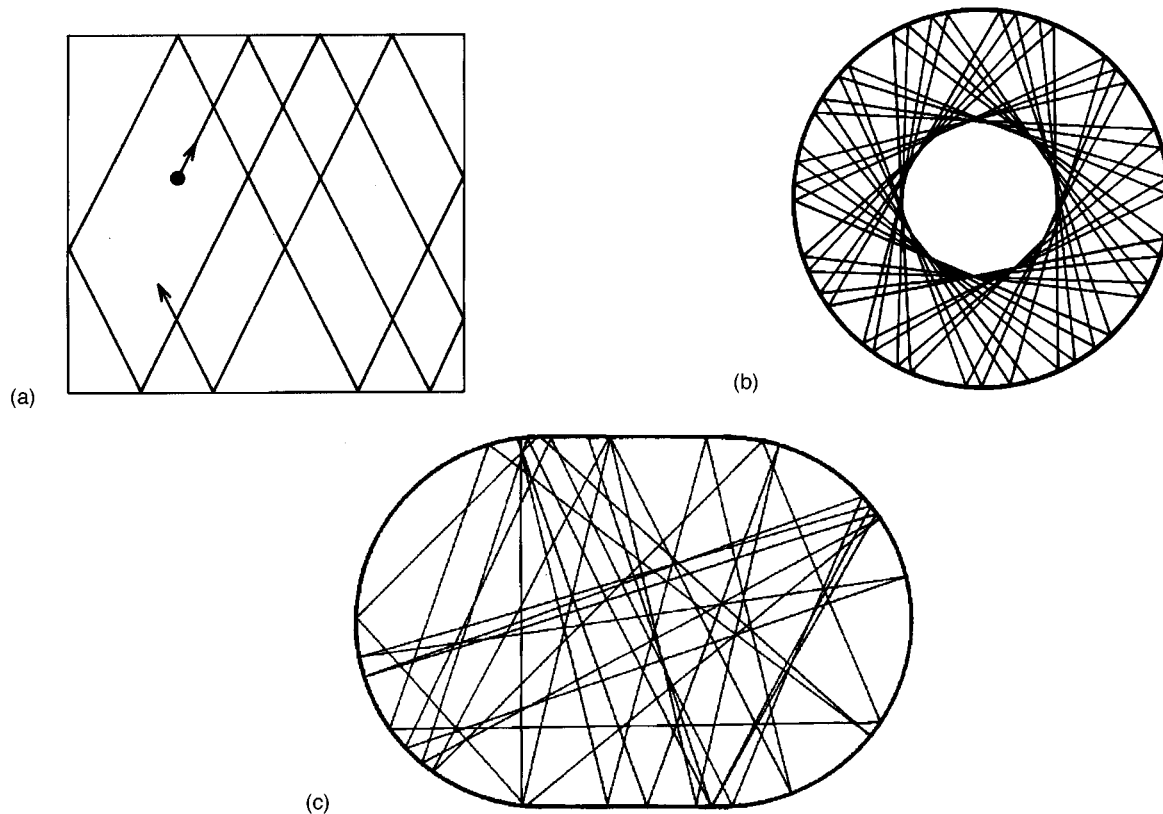


Fig. 2. Typical trajectories in billiards: (a) in the rectangle, (b) in the circle (this trajectory shows a caustic), and (c) in the Bunimovich stadium.

grable billiards can be modeled in a classroom with an analog experiment. The experimental setup basically contains a function generator and a mechanical vibrator and is based on the vibrations of a soap film.⁸ Thus, as Feynman said in 1963, “the same equations have the same solutions.”⁹

In the next section we briefly discuss classical and quantum billiards. In Sec. III we introduce our experimental setup and show the analogy with the quantum billiard. Other uses of our experimental setup are discussed in the same section. Some remarks are given in the conclusion.

II. CLASSICAL AND QUANTUM BILLIARDS

In order to make a more explicit definition of the classical billiard we take a two-dimensional region denoted by R and define the potential V for the particle as

$$V = \begin{cases} 0 & \text{in } R \\ \infty & \text{otherwise.} \end{cases} \quad (1)$$

This means that inside R the particle is free and moves in straight lines. When the particle collides with the boundary, it bounces following the law of reflection. Under this dynamics, the rectangle and circle billiards are regular. Typical trajectories inside are shown in Fig. 2. On the other hand, the dynamics of a particle in the stadium as well as in the Sinai billiard, are chaotic. Almost all trajectories for these billiards are ergodic and exponentially divergent. Roughly speaking, this is so because in the Sinai billiard, two very close trajectories are separated when one collides (or both) with the central circle. After some time, the separation between the trajectories (in phase space) is exponential. In the stadium, two particles with very close initial conditions are focused

when they collide with one semicircle. After this focusing, they began to separate until they bounce again but now on the other semicircle. The exponential divergence appears because the separation time is greater than the focusing time. Apart from these trajectories there also exist periodic orbits. These trajectories are unstable and typically isolated. Their

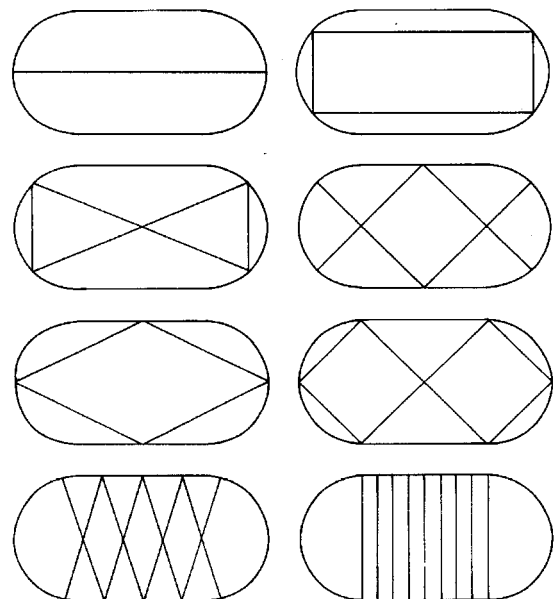


Fig. 3. Periodic orbits in the Bunimovich stadium. Notice that in some cases more than one orbit is present and that all obey the reflection law.

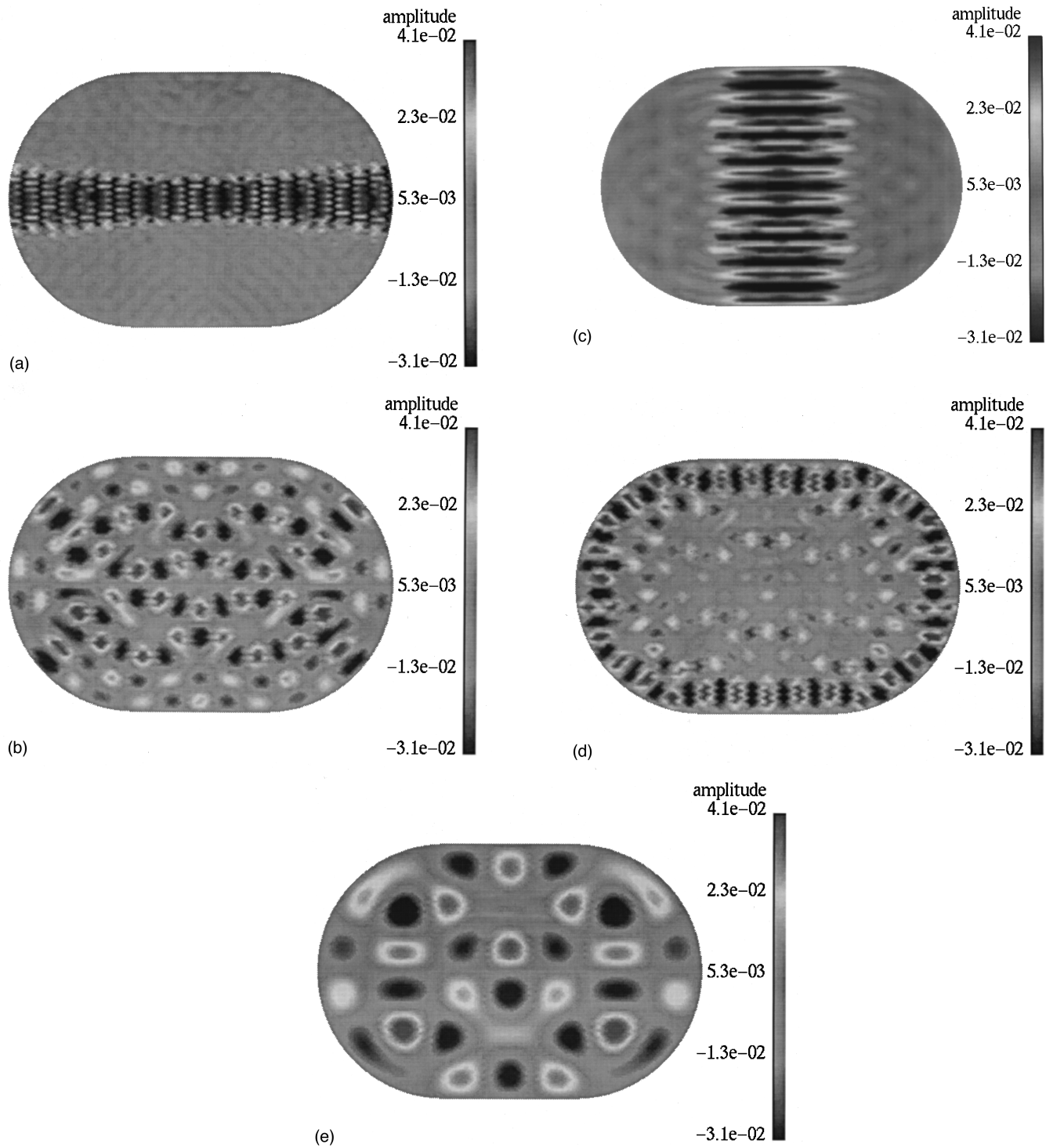


Fig. 4. Eigenfunctions of the Bunimovich stadium calculated by the finite element method for a quadrant of stadium with Dirichlet boundary conditions. The maxima and minima of each normal mode correspond to the darkest zones; (a) a typical state scarred by a short classical orbit connecting the two extremes of the stadium, (b) a state scarred by an orbit of large period, (c) a typical state scarred by a “bouncing-ball” orbit, (d) a “whispering gallery” state, and (e) a typical noisy state if one looks only at a quadrant.

number increases exponentially as a function of their length, but they are of measure zero in phase space. We may find also families of unstable and non-isolated periodic orbits such as the “bouncing-ball” orbits in which the particle bounces between the two parallel segments of stadium. Some periodic orbits for the Bunimovich stadium are shown in Fig. 3.

The time-independent Schrödinger equation for the potential defined in Eq. (1) is

$$\nabla^2 \Psi + k^2 \Psi = 0 \quad \text{in } R \quad (2)$$

$$\Psi = 0 \quad \text{on the boundary of } R,$$

with the wave number $k = (2mE/\hbar^2)^{1/2}$. Here, E and m are the energy and mass of the particle and \hbar is the Planck constant. The homogeneous Dirichlet boundary condition is obtained because if $V = \infty$ the wave function vanishes. The Helmholtz equation in R and the Dirichlet boundary condition define the quantum billiard. Note that this is just the equation for the normal modes of a membrane if we interpret the functions as vibration amplitudes.

For classically integrable billiards, the eigenfunctions are well-known. For example, the solutions for circular and rectangular billiards are Bessel functions and sinusoidal functions, respectively.¹⁰ On the other hand, the features of wave functions for classically chaotic billiards have been well-studied numerically by Heller.⁷ Recently, experiments in microwave cavities have been performed.¹¹ In Fig. 4 we show eigenfunctions of the Bunimovich stadium we calculated numerically using the finite element method.¹² However, they can alternatively be calculated by standard software. The eigenfunctions of Fig. 4(a)–(c) show certain similarities with the orbits of Fig. 3. Following Heller, we say that the eigenfunctions are “scarred” by the orbits. Figure 4(d) shows what is called a “whispering gallery” state, because there exist certain galleries¹³ in which the sound travels inside them, following the border. This kind of state is associated with orbits also close to the boundary. The eigenfunction shown in Fig. 4(e) resembles noise⁴ when we see only a quarter of stadium.

The appearance of the scars is quite well understood¹⁴ based on the theoretical work by Selberg, Gutzwiller, and Balian.¹⁵ Due to the low density of the short periodic orbits, they may well be seen in quantum experiments and simulations either as dominant features in the Fourier spectrum or as scars. While the Fourier analysis of experimental data in atomic¹⁶ and molecular physics¹⁷ is quite striking, direct demonstrations of scars are difficult even in microwave cavities. A simple explanation of scarring is based on de Broglie waves. Close to the periodic orbit there exist standing de Broglie waves whose wavelength λ is associated with the length L of the periodic orbit:

$$2L = n\lambda, \quad n = 1, 2, 3, \dots \quad (3)$$

These de Broglie waves are localized around periodic orbits due to the exponential divergence of nearing trajectories. In the next section we will show how a simple demonstration setup can display the most interesting features of the eigenfunctions on a soap film.

III. SOAP FILM ANALOGY

The normal modes of a rectangular and circular soap film have been well studied.^{18–20} A textbook showing these eigenfunctions is French’s book entitled *Vibrations and Waves*.²¹ The governing equation is the time-independent wave Eq. (2), but now with a different interpretation: Ψ is the membrane vibration amplitude and the wave number is now $k = \omega/v$, with ω the angular frequency and v the speed of the transverse waves on the membrane.

A problem arises for the experimental setup of this analog: At high frequencies (corresponding to the semiclassical limit), the damping is large. To solve this problem we feed energy into the system permanently with an external resonator of a well-defined but variable frequency. We chose to feed the external frequency into the system by vibrating the wire that delimits our soap film. We use a mechanical vibra-



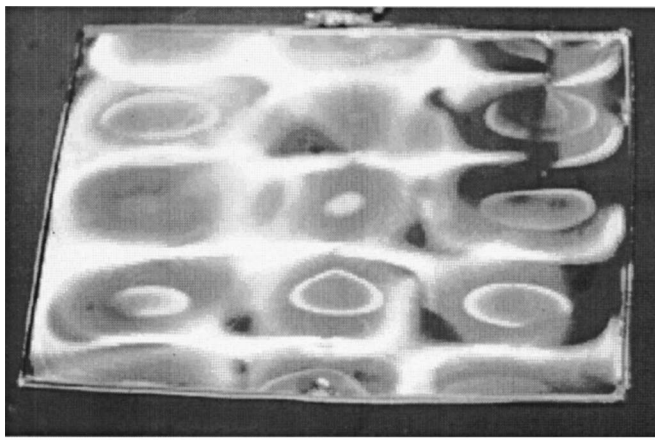
Fig. 5. Experimental setup used to show the quantum features of chaos. Notice that the membrane is excited in a way that breaks the symmetry.

tor (PASCO Scientific model SF-9324, see Fig. 5) connected to a function generator (we used a generator Wavetek model 18022) and used wires with different shapes (rectangle, circle, Bunimovich stadium, Sinai billiard, and some others of interest²³). Alternatively a speaker could be used to transmit the frequency through the air.^{19,20,24} The chemical formula for a soap film with large duration is given by Walker,²⁴ but can be made up with soap, water, and glycerin by trial and error.

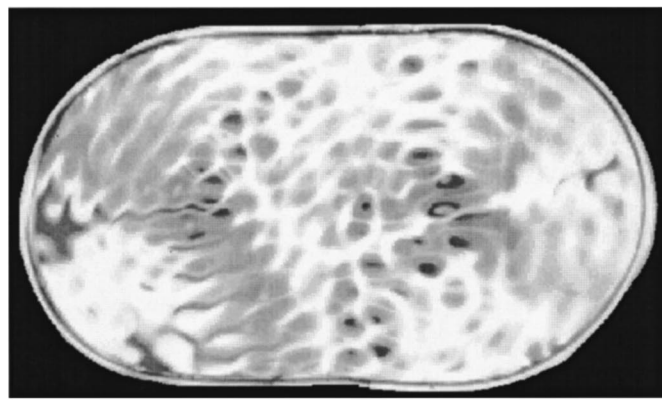
We can now start the demonstration. In Fig. 6(a) we show a normal mode of the rectangle, in agreement with the known result. Figure 6(b) shows a normal mode for a circle displaying a Bessel function. Roughly speaking, the shining and dark zones establish a periodic pattern associated with the normal mode. Although the pattern established cannot give a quantitative measure of the amplitude, it is sufficient to give an idea of the form of the normal mode and to identify it. However, the more interesting normal modes are some of the classically chaotic billiards. In Fig. 6(c) we show a “bouncing-ball” state at low energies for a Bunimovich stadium. The alternating dark and shining zones in this and in the following figures make evident the presence of standing waves in the membrane. These waves are associated with de Broglie waves in the quantum billiard and at the same time they are associated with periodic orbits in the classical billiard. In Fig. 6(d) and (e) scarred eigenfunctions are displayed, the latter in the high-frequency regime. In order to show that they are scars and not some spurious effect of our very simple experimental setup, we calculate numerically the normal modes at frequencies near the experimental ones. We observe in Fig. 4 some of these eigenfunctions and the corresponding orbits in Fig. 3.

We want to mention that the normal modes in soap films can also be used for other two-dimensional wave phenomena, such as the search for normal modes of the clay layer corresponding to the old Tenochtitlan lake, which plays a crucial role in the earthquake damage patterns of Mexico City.²⁵ The application in this case comes from the fact that the upper clay layer of the Mexico Valley, as well as the soap films, are practically two-dimensional.²⁵ A wire may readily be shaped to the corresponding boundary and the results are shown in Fig. 6(f).

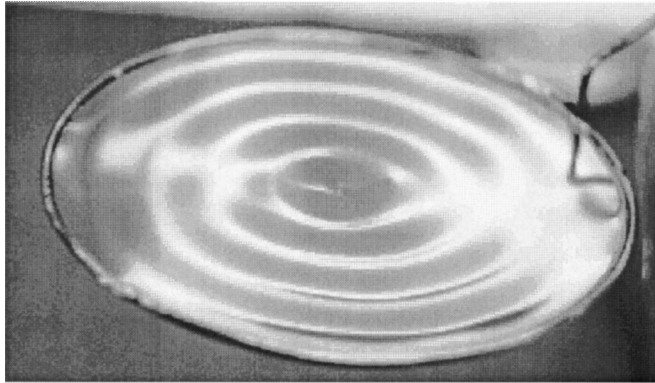
Moreover, the experimental setup which we present may be used to show other related wave phenomena. Typical examples are scars on liquids,²⁶ Faraday waves—crystallographic patterns in large-amplitude waves²⁷—quasicrystalline patterns on liquids,²⁸ sand dynamics,²⁹ or



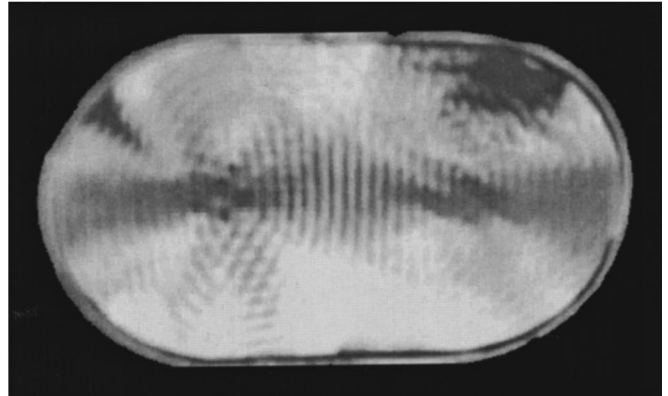
(a)



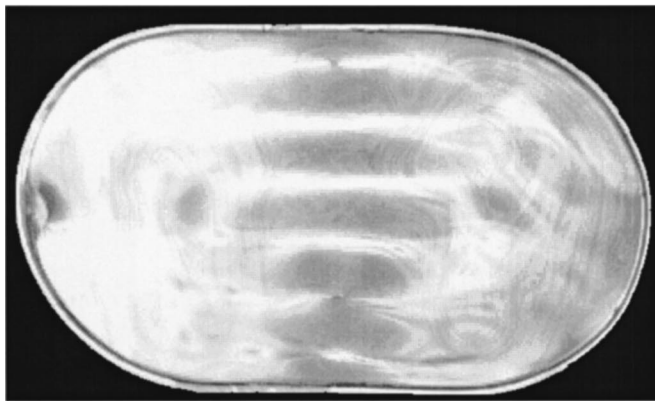
(d)



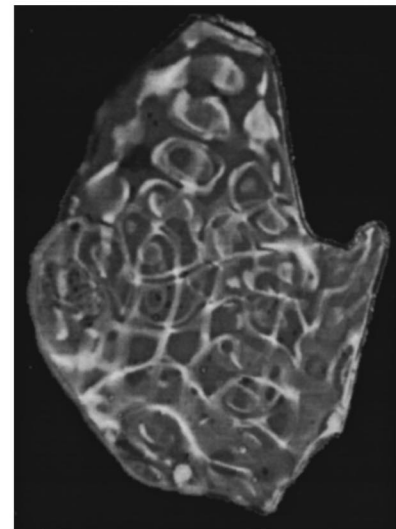
(b)



(e)



(c)

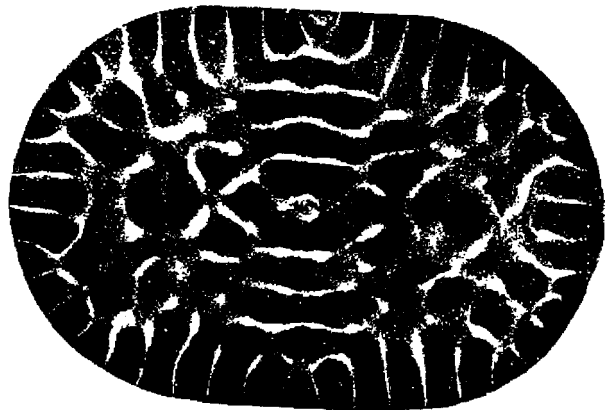


(f)

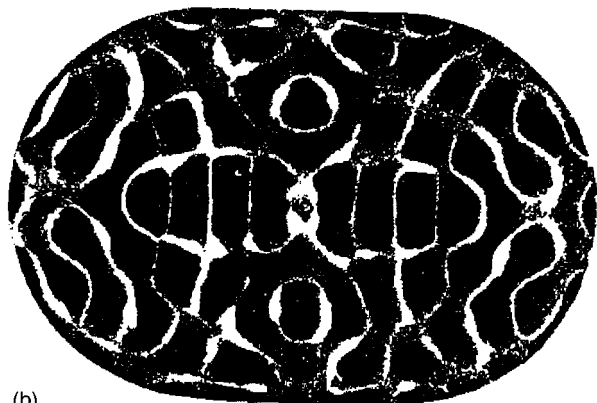
Fig. 6. Normal modes for different shapes. (a) Low mode for the rectangle at a frequency of 22.48 Hz. (The frequency changes slightly for different soap solutions and different thicknesses of the soap film.) The rectangle is of size $0.215\text{ m} \times 0.155\text{ m}$. (b) Bessel function for a circular-shape wire. The radius of the wire is 0.092 m and the excitation frequency is around 33.5 Hz. (c) A “bouncing-ball state” close to 40 Hz. (d) A scarred state corresponding to the numerical one shown in Fig. 4(b) at a frequency close to 110 Hz. (e) A scarred state by a short classical orbit connecting the two extremes of the stadium for a Bunimovich stadium with $r=0.035\text{ m}$ and $d=0.035\text{ m}$. The corresponding frequency is about 478 Hz. (f) The normal mode for a wire with “old Tenochtitlan lake” form at frequency $\nu=48.88\text{ Hz}$.

normal modes of Chladni’s plates.³⁰ These can be done by replacing the wire in our experimental setup with water containers or thin plates. If we want to see scars on surface waves, we must use a stadium-shaped tank filled with water. Faraday waves can be obtained by adding shampoo to the

water and increasing the amplitude and frequency but decreasing the level of the liquid to several millimeters. It is not necessary to use tanks with different shapes because the patterns do not depend on the boundary. If we want to observe quasicrystalline patterns with this experimental setup,



(a)



(b)

Fig. 7. Nodal patterns observed on iron plates with stadium shape. The plate was of 1 mm thickness and we used $r=0.1$ m and $d=0.1$ m. (a) A whispering gallery at 5.79 kHz. Notice that this pattern is better defined near the boundary and between the two segments of the stadium. This means that the amplitudes are higher in these regions. (b) A scar which reflects the orbit connecting the two extremes of the stadium. In this case the pattern is better defined on the periodic orbit. The frequency for this case was around 4.22 kHz.

we must excite the mechanical vibrator with—at least—two frequencies.²⁸ This is easily obtained by changing the sinusoidal time dependence of the driving force to a triangular one.³¹ Another application is the demonstration of the modes of thin plates. In this case, as well as in the water tanks, the whispering gallery states are easily visible. We may use ellipses, pentagons, or any other shape. All these plates are excited at a point at which the mechanical vibrator loads them. Figure 7(a) shows a whispering gallery state for a stadium-shaped iron plate. Figure 7(b) shows a scarred pattern for the same plate. Finally, if we consider a tank with a layer of sand of variable thickness, we may study several topics on dynamics of granular media. As an example we can study “standing waves” on sand.²⁹

IV. CONCLUSIONS

The analog model of soap films for the quantum billiard gives a demonstration of quantum chaos features. For integrable regions the normal modes correspond to the eigenfunctions of a two-dimensional square box and a circle. For classically chaotic billiards the normal modes correspond to scarred eigenfunctions in the semiclassical limit. The experimental setup presented here is particularly cheap, simple,

and elegant—i.e., the alternative experiments do not satisfy the Helmholtz equation and/or boundary condition. Microwave cavities are expensive and do not display the scars in a directly visible manner. Thus the simplicity of the experimental setup and the facility to use any shape makes it very suitable for the undergraduate laboratory. Furthermore the normal modes of soap films can be used to demonstrate other two-dimensional analog phenomena. Finally, we want to mention that the proposed experimental setup can be quickly changed to study other related wave phenomena. A wide variety of highly nontrivial wave-like phenomena can be displayed with minimal experimental requirements.

ACKNOWLEDGMENTS

We want to thank T. H. Seligman, F. Leyvraz, and J. A. Heras for their valuable comments. Also we would like to thank the C. O. F., Física General and Física Moderna Laboratories of the Facultad de Ciencias U.N.A.M., especially Felipe Chávez. Finally, we thank L. M. de la Cruz for his useful help with some of the figures. The numerical work was done with the Cray supercomputer of U.N.A.M.

^{a)}Electronic mail: mendez@ce.ifisicam.unam.mx

¹B. V. Chirikov, “A universal instability of many-dimensional oscillator systems,” *Phys. Rep.* **52**, 263–379 (1979).

²O. Bohigas, M. J. Giannoni, and C. Schmit, “Characterization of chaotic quantum spectra and universality of level fluctuation laws,” *Phys. Rev. Lett.* **52**, 1–4 (1984). See also “Spectral fluctuations of classically chaotic quantum systems,” in *Quantum Chaos and Statistical Nuclear Physics*, edited by T. H. Seligman and H. Nishioka (Springer, Berlin, Heidelberg, New York, 1986), pp. 18–40.

³T. H. Seligman, J. J. M. Verbaarschot, and M. R. Zirnbauer, “Quantum spectra and transition from regular to chaotic classical motion,” *Phys. Rev. Lett.* **53**, 215–217 (1984). See also “Spectral fluctuation properties of Hamiltonian systems: The transition between order and chaos,” *J. Phys. A* **18**, 2751–2770 (1985).

⁴For a pedagogical paper on quantum chaos, see M. V. Berry, “Semiclassical mechanics of regular and irregular motion,” in *Chaotic Behavior of Deterministic Systems*, Les Huoches Lectures XXXVI, edited by R. H. Helleman and G. Iooss (North-Holland, Amsterdam, 1985), pp. 171–271.

⁵M. C. Gutzwiller, *Chaos in Classical and Quantum Mechanics* (Springer-Verlag, New York, 1990), pp. 196.

⁶Eric J. Heller and Steven Tomsovic, “Postmodern quantum mechanics,” *Phys. Today* **46** (7), 38–46 (1993).

⁷E. J. Heller, “Qualitative properties of eigenfunctions of classically chaotic Hamiltonian systems,” in *Quantum Chaos and Statistical Nuclear Physics*, edited by T. H. Seligman and H. Nishioka (Springer, Berlin, Heidelberg, New York, 1986), pp. 162–181, and references therein.

⁸Both the Schrödinger equation for a billiard and the wave equation for a membrane are reduced to the Helmholtz equation when the time-independent part is taken. Nevertheless, to deduce the wave equation for the membrane air, gravity, and damping in the high frequency regime are usually neglected.

⁹Richard P. Feynman, Robert B. Leighton, and Matthew Sands, *The Feynman Lectures on Physics Mainly Electromagnetism and Matter*, Vol. II (Addison-Wesley, Reading, MA, 1964), pp. 12–1.

¹⁰K. F. Graff, *Wave Motions in Elastic Solids* (Dover, New York, 1991, reprint), pp. 225–229.

¹¹S. Sridhar, “Experimental observation of scarred eigenfunctions of chaotic microwave cavities,” *Phys. Rev. Lett.* **67**, 785–788 (1991).

¹²M. Mori, *The Finite Element Method and its Applications* (MacMillan, New York, 1983).

¹³St. Pauls in U.K. is an example.

¹⁴E. B. Bogomolny, “Smoothed wave functions of chaotic quantum systems,” *Physica D* **31**, 169–189 (1988).

¹⁵These authors developed a formula according to which a solution to quantum problems may be written as a sum over all periodic orbits of its classically chaotic counterpart. This formula is exceedingly complicated due to the exponential increase of the number of such orbits as a function of their length. On the other hand, the shortest orbits are few and display

- some typical features of the problem. There are textbooks on classical and quantum chaos containing discussions of the Selberg–Gutzwiller–Balian periodic orbits sum expression. See, for example, L. E. Reichl, *The Transition to Chaos* (Springer-Verlag, New York, 1992), pp. 318–381. See also M. C. Gutzwiller, Ref. 5, pp. 282–321.
- ¹⁶A. Holle, J. Main, G. Wiebusch, H. Rotke, and K. H. Welge, “Quasi-Landau spectrum of the chaotic diamagnetic hydrogen atom,” *Phys. Rev. Lett.* **61**, 161–164 (1988).
- ¹⁷M. Lombardi and T. H. Seligman, “Universal and nonuniversal statistical properties of levels and intensities for chaotic Rydberg molecules,” *Phys. Rev. A* **47**, 3571–3586 (1993).
- ¹⁸Cyril Isenberg, *The Science of Soap Films and Soap Bubbles* (Tieto, Clevedon, Avon, England, 1978). This book gives an excellent account of the many properties of soap films and soap bubbles. It also contains an extensive list of references on the subject.
- ¹⁹D. T. Kagan and L. J. Buchholtz, “Demonstrations of normal modes on a bubble membrane,” *Am. J. Phys.* **58**, 376–377 (1991).
- ²⁰L. Bergmann, “Experiments with vibrating soap membranes,” *J. Acoust. Soc. Am.* **28** (6), 1043–1047 (1956).
- ²¹A. P. French, *Vibrations and Waves* (Norton, New York, 1971), pp. 185–186.
- ²²The generator and mechanical vibrator can be used for other vibrating systems. See, for instance, Christopher C. Jones, “A mechanical resonance apparatus for undergraduate laboratories,” *Am. J. Phys.* **63**, 232–236 (1995).
- ²³The possibility to introduce a billiard of any shape easily is the great advantage of the experimental setup which we present. Domains with different shape but the same spectrum may be studied. See, for instance, H. Weidenmüller, “Why different drums can sound the same,” *Phys. World* (22–23 August 1994). Other billiards associated with classically chaotic or integrable billiards may be studied. This is the case of the ellipse billiard, the oval billiard, the triangle billiard (all kinds of triangles), polygonal billiards, etc., and in general, billiards constructed in order to obtain some special feature of classically chaotic systems such as special discrete symmetries.
- ²⁴J. Walker, “Music and ammonia vapor excite the color pattern of a soap film,” *Sci. Am.* **257** (2), 92–95 (1987).
- ²⁵J. Flores, O. Novaro, and T. H. Seligman, “Possible resonance effect in the distribution of earthquake damage in Mexico City,” *Nature* (London) **326**, 783–785 (1987).
- ²⁶R. Blümel, I. H. Davidson, W. P. Reinhart, H. Lin, and M. Sharnoff, “Quasilinear ridge structures in water surface waves,” *Phys. Rev. A* **45**, 2641–2644 (1992).
- ²⁷G. M. Zaslavsky, R. Z. Sagdeev, D. A. Usikov, and A. A. Chernikov, *Weak Chaos and Quasi-Regular Patterns* (Cambridge U.P., New York, 1991), pp. 170–187.
- ²⁸S. Fauve, “Parametric instabilities,” in *Dynamics of Nonlinear and Disordered Systems*, edited by G. Martínez-Meckler and T. H. Seligman (World Scientific, Singapore, 1995), pp. 67–115.
- ²⁹F. Melo, P. Umbanhowar, and H. L. Swinney, “Transition to parametric wave patterns in a vertically oscillated granular layer,” *Phys. Rev. Lett.* **72**, 172–175 (1994).
- ³⁰J. Stein and H.-J. Stöckmann, “Experimental determination of billiard wave functions,” *Phys. Rev. Lett.* **68**, 2867–2870 (1988).
- ³¹J. Bechhoefer and B. Johnson, “A simple model for Faraday waves,” *Am. J. Phys.* **64**, 1482–1487 (1996).